



Ultramafic-derived arsenic in a fractured bedrock aquifer

Peter C. Ryan^{a,*}, Jonathan Kim^b, Andrew J. Wall^c, Jonathan C. Moen^a, Lilly G. Corenthal^a, Daniel R. Chow^a, Colleen M. Sullivan^a, Kevin S. Bright^a

^a Geology Department, Middlebury College, 276 Bicentennial Way, Middlebury, VT 05753, USA

^b Vermont Geological Survey, Waterbury, VT 05671, USA

^c Department of Geosciences, Penn State University, University Park, PA 16802, USA

ARTICLE INFO

Article history:

Available online 6 January 2011

ABSTRACT

In the fractured bedrock aquifer of northern Vermont, USA, As concentrations in groundwater range from <1 to 327 µg/L (<13–4360 nm/L) and these elevated occurrences have a general spatial association with ultramafic rock bodies. The ultramafic rocks in this region are comprised mainly of serpentinites and talc–magnesite rocks with average As concentration of 93 ppm and a range from 1 to 1105 ppm. By comparison, the other main lithologies in the study area are depleted in As relative to the ultramafics: the average As concentration in metabasaltic rocks is 4.1 ppm with a range of <1–69 ppm, and mean As concentration in meta-sedimentary phyllites and schists is 22 ppm with a range of <1–190 ppm. In the ultramafic rocks, As is correlated with Sb and light rare earth elements, indicating that As was introduced to the ultramafic rocks during metasomatism by fluids derived from the subducting slab. Evidence from sequential chemical extraction, X-ray diffraction (XRD) and stoichiometric analysis indicates that the majority of the As is located in antigorite and magnesite (MgCO₃) with lesser amounts in magnetite (Fe₃O₄). Hydrochemistry of monitoring wells drilled into fractured ultramafic rock in a groundwater recharge area with no anthropogenic As source reveals above background As (2–9 µg/L) and an Mg–HCO₃ hydrochemical signature that reflects dissolution of antigorite and magnesite, confirming that As in groundwater can be derived from ultramafic rock dissolution. Arsenic mobility in groundwater affected by ultramafic rock dissolution may be enhanced by alkaline pH values and relatively high HCO₃⁻ concentrations.

© 2011 Elsevier Ltd. All rights reserved.

1. Introduction

The mineralogical source of As in alluvial and bedrock aquifers is an important factor controlling the potential for mobilization of As into drinking water, particularly in bedrock aquifers where As-bearing minerals are likely to be heterogeneously distributed (Robinson and Ayotte, 2006). For example, in southern New Hampshire, USA, groundwater with elevated As is associated with Devonian pegmatites which are concentrated in As relative to other lithologic units (Peters and Blum, 2003), and in eastern Maine, USA, As is primarily derived from sulfidic schist (Lipfert et al., 2006), but the amount of As in meta-sedimentary rocks decreases with increasing metamorphic grade (O'Shea et al., 2008, 2009). High As groundwaters are spatially associated with Au-bearing sulfide–quartz veins in Burkina Faso and Alaska (Smedley et al., 2007; Verplanck et al., 2008), and in Triassic sandstones of Germany, where As concentrations in groundwater are correlated with sedimentary facies (Heinrichs and Udluft, 1999). In these systems, determining lithologic or facies associations of the As-bearing

minerals yields valuable information on spatial distribution as well as dissolution and transport mechanisms of As in the aquifer.

More generally, the mineralogical and geochemical properties of As parent minerals affect thermodynamic stability, rate of dissolution, speciation of As released into solution and potential for As sequestration; similarly, characteristics of the aqueous system will mobilize As from different mineralogical hosts under different conditions. For example, decomposition of Fe sulfides in oxidized groundwater typically results in formation of Fe-hydroxides which sequester As as arsenite or arsenate in inner-sphere complexes (Fendorf et al., 1997; Arai et al., 2004). Conversely, chemically-reducing groundwaters facilitate reductive dissolution of Fe-hydroxides, leading to release of sorbed As into solution (Smedley and Kinniburgh, 2002; Mukherjee et al., 2008). In the presence of mildly acidic solutions, hydrolysis reactions tend to enhance dissolution of minerals like carbonates and Mg silicates, so As associated with these types of minerals would be prone to mobilization under these conditions.

Sulfide minerals, particularly As-bearing pyrite, are most commonly cited as the primary source of As in groundwater (Acharyya et al., 1999; Nordstrom, 2002; Smedley and Kinniburgh, 2002). However, O'Shea et al. (2008, 2009) indicate that while As occurs in pyrite in low-grade metamorphic

* Corresponding author. Tel.: +1 802 443 2557.

E-mail address: pryan@middlebury.edu (P.C. Ryan).

bedrock aquifers of eastern Maine (USA), it is virtually absent in stratigraphically equivalent medium- and high-grade metamorphic rocks, suggesting that mobile As is driven from these rocks during metamorphism above greenschist grade (Bebout et al., 1999). Silicate minerals, while abundant in aquifers, typically only contain trace amounts of As and are not usually thought to be sources of elevated As in groundwater (Smedley and Kinniburgh, 2002), although a few recent articles suggest that in some cases, minerals such as antigorite or biotite may contain elevated As and hence play important roles as As sources (Hattori et al., 2005; Guillot and Charlet, 2007; Seddique et al., 2008). Carbonates are common aquifer minerals that are known to be able to fix As (Horton et al., 2001; Di Benedetto et al., 2006; Alexandratos et al., 2007) yet have not been regarded as significant As sources in groundwater. Minerals such as arsenides (e.g. nicolite) and As sulfides (e.g. arsenopyrite, realgar and orpiment), while rich in As, are rare in the natural environment and typically are not important sources of As in aquifers (Smedley and Kinniburgh, 2002; Nordstrom, 2002; Nordstrom and Zheng, 2009). Iron-hydroxides have been recognized at many localities as the solid-phase source of As in groundwater wells, but as pointed out by Seddique et al. (2008), they are secondary phases that form during weathering or diagenetic alteration, and in many cases, the primary mineralogical source of As is unknown.

In this article, attention is drawn to the potential for serpentinite-derived As in groundwater, a possibility that has been recently suggested by two lines of evidence: (1) X-ray absorption analyses of Himalayan serpentinites by Hattori et al. (2005) which indicated the presence of As in antigorite; and (2) the occurrence of groundwater with elevated As (<1–327 µg/L; <13–4360 nm/L) that exhibits a general spatial association with As-rich serpentinite and talc-magnesite rocks in northern Vermont, USA (Bright, 2006; Sullivan, 2007; Chow, 2009; Corenthal, 2010). Guillot and Charlet (2007) argued that As-rich serpentinites in the Himalayan source area may be the primary As source in As-affected aquifers of the West Bengal–Bangladesh system. In rural northern Vermont, analysis of land use history and geochemical signatures of groundwater have ruled out potential anthropogenic sources such as Pb arsenate pesticides, landfill plumes and industrial emissions (Bright, 2006; Sullivan, 2007) and hydrochemical analysis of groundwater in monitoring wells reveals a Mg–HCO₃ signature (Chow, 2009) that is typical of waters influenced by antigorite or magnesite dissolution (Barnes and O’Neil, 1969).

Accordingly, the purpose of this article is to evaluate the mineralogy and geochemistry of As-rich serpentinites and talc-magnesite rocks in northern Vermont, to relate these findings to groundwater chemistry, and to test the hypothesis that these metasomatically-altered ultramafic rocks are the source of the elevated As in bedrock and alluvial aquifers. On a broader scale, the presence of serpentinites and related ultramafic rocks in tectonic suture zones globally, combined with the recent suggestion that serpentinites may be the primary source of As in the Bengal fan (Guillot and Charlet, 2007), indicate that the results of this study may have implications for determining primary sources of As and also for predicting areas with potential for elevated groundwater As (i.e. suture zones with serpentinites or alluvium derived from these settings).

2. Regional geology and background

The study area is located in the northern Appalachians of northern Vermont, bordered to the north by the USA–Canada border, to the south by the Winooski River valley near Waterbury, to the west by the foothills of the Green Mountains (Mount Mansfield northward to Jay Peak), and to the east by the foothills of the Worcester Range and Lowell Mountains (Fig. 1). This region is approximately

800 km² in area and is characterized by a narrow sediment-filled valley with localized bedrock outcrops with generally ≤100 m of local relief within the valley. These bedrock knobs are often covered by a mantle of glacial till with only sparse outcrops. The Misisquoi River is the main stream in the northern part of the study area while the Winooski River is the largest stream in the southern part of the study area.

Rock types that comprise the regional fractured bedrock aquifers in the study area occur within the Rowe–Hawley Belt (RHB), a sequence of Ordovician phyllite (metamorphosed shales and sandstones), greenstone (metabasalt) and isolated pods of serpentinite and associated ultramafic rocks (Fig. 1)—these rocks comprise a tectonic assemblage of thrust slices originally juxtaposed in the suture zone for the Ordovician Taconian Orogeny (Stanley and Ratcliffe, 1985).

Within the RHB, ultramafic rocks commonly occur as elongate bodies within fault-bounded sequences and represent vestiges of metasomatically-altered suprasubduction zone mantle peridotite (Coish and Gardner, 2004). Although the highly serpentinitized peridotites in northern Vermont are not part of a well-developed ophiolite sequence in the study area, they occur along strike with the Thetford Mines ophiolite to the north in Quebec (Doolan et al., 1982) and geochemical evidence indicates that the Vermont ultramafics represent ophiolitic remnants (Coish and Gardner, 2004). These rocks were emplaced into continental crust during continent–arc collision associated with the Taconian Orogeny that followed eastward subduction of the Laurentian (North American) margin under an encroaching arc (Stanley and Ratcliffe, 1985). Detailed models of the generation, alteration and emplacement of the Vermont ultramafics are presented in Cady et al. (1963), Chidester et al. (1978), Labotka and Albee (1979), Van Baalen et al. (1999) and Coish and Gardner (2004).

The meta-sedimentary rocks in the study area are dominated by phyllites of the Proterozoic-to-Cambrian Hazens Notch and Stowe formations, the Cambrian Ottaqueechee Formation and the late Cambrian to Ordovician Moretown Formation; these rocks originated as marine sediments deposited on the distal continental shelf and rise and, in the case of the Moretown Formation, a forearc basin. They then were incorporated into an accretionary prism during eastward-dipping subduction in the Ordovician (e.g., Stanley and Ratcliffe, 1985; Kim and Jacobi, 1996) and subsequently metamorphosed at greenschist facies conditions; these rocks now occur in fault contact with each other and with the serpentinitized ultramafics. Greenstones and amphibolites also occur along fault-bounded slivers within the study area—these are metamorphosed basaltic volcanic rocks that formed at mid-ocean ridge, rift or back-arc basin settings (Coish et al., 1986; Coish, 1997; Kim et al., 2003; Morris, 2006).

Elevated As has been observed in the Rowe–Hawley Belt in fractured crystalline bedrock aquifers (Bright, 2006; Chow, 2009) as well as aquifers in surficial deposits of glacial till and outwash that contain ultramafic clasts (Corenthal, 2010). The entire region was inundated by the Laurentide Ice Sheet during the late Pleistocene, producing valley-fill deposits of till and outwash and a mantle of glacial till on bedrock knobs and hillslopes (Stewart and MacClintock, 1969). In areas where valley-fill deposits are sufficiently thick, groundwater is produced from interstratified till and glacial outwash, and where only a thin mantle of till or exposed bedrock is present, groundwater is produced from fractured bedrock of the RHB.

Given the rural nature of Vermont, approximately 50% of the population produces drinking water from private, unregulated wells, and the goal of a series of research projects has been to examine regional trends in rural groundwater As (Bright, 2006; Sullivan, 2007; Chow, 2009; Corenthal, 2010). Results indicate that many wells in the ultramafic belt contain values in excess of 10 µg/L

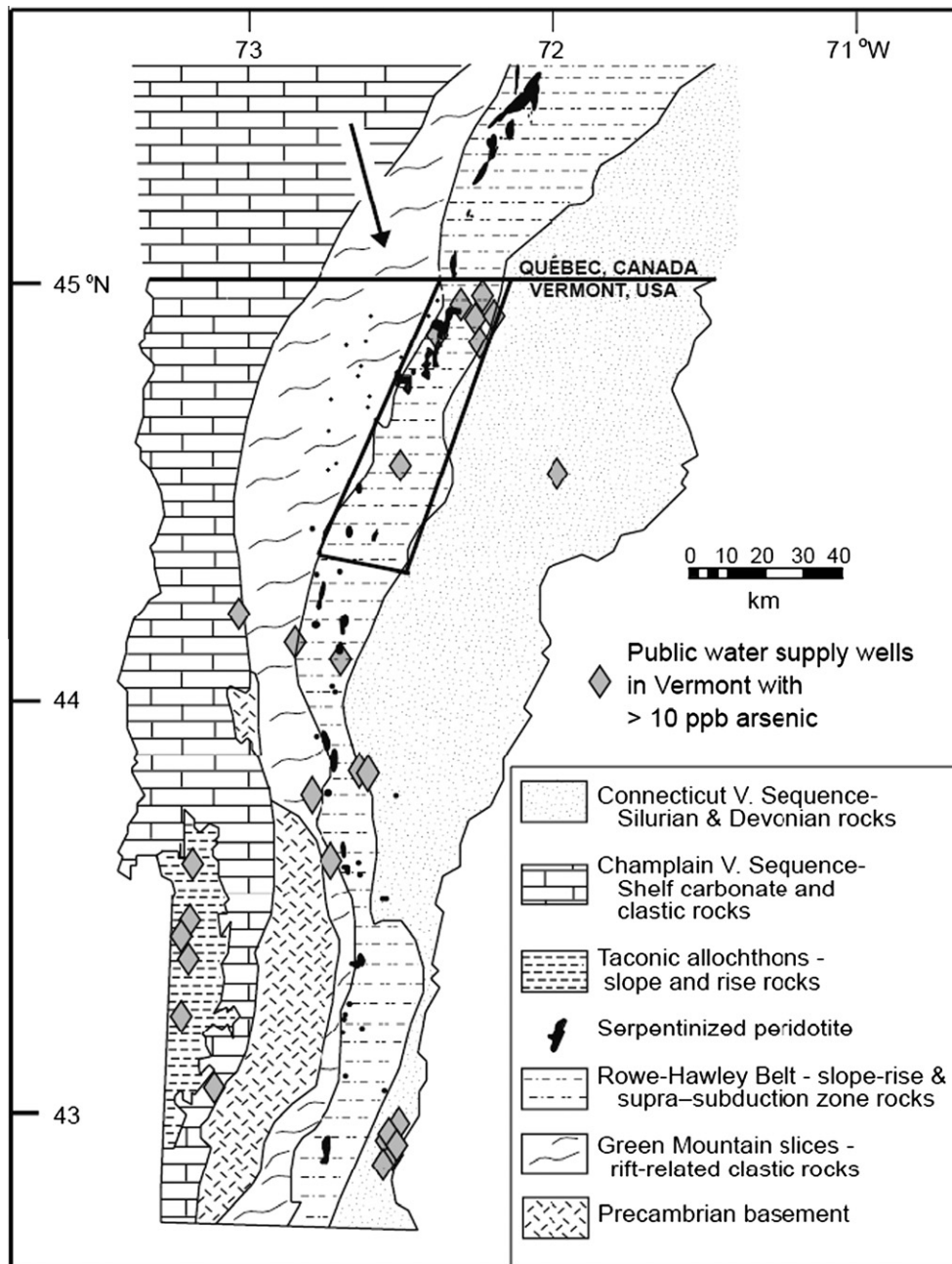


Fig. 1. Generalized geologic map of Vermont and adjacent southern Québec (after Doll et al., 1961; Shiels and Smith, 1989; Stanley and Ratcliffe, 1985; Kim et al., 2003; Schroetter et al., 2006). Rock and water samples were obtained from within the area outlined by the trapezoid in the north-central part of Vermont. Public water supplies in Vermont that exceed the USEPA maximum contaminant level of 10 ppb are also shown.

(133 nm/L)—of 45 wells analyzed from this area, 27% (12/45) contained $>10 \mu\text{g/L}$ As (Bright, 2006; Chow, 2009; Corenthal, 2010). The mean As concentration in these wells is $16.5 \mu\text{g/L}$, with a range of <1 –327. In order to calculate means where some values are less than the detection limit, the value of the detection limit was used for non-detects (Cloutier et al., 2006); for the above-cited groundwater As mean, if the value used for samples below detection limit ($1 \mu\text{g/L}$) is replaced by zero, the mean changes slightly from $16.5 \mu\text{g/L}$ to $15.9 \mu\text{g/L}$. It is also worth noting that there is great heterogeneity in the groundwater As values. The mean is skewed by three wells with high values of 93, 113 and $327 \mu\text{g/L}$; nine wells contain between 10 and $38 \mu\text{g/L}$ As, seven wells contain 1– $10 \mu\text{g/L}$ and 26 wells contain $<1 \mu\text{g/L}$.

3. Materials and methods

3.1. Whole-rock geochemistry

One hundred and seven samples of bedrock were collected from numerous outcrop sites and three monitoring wells (cuttings sampled at 1.5 m intervals) to obtain a representative suite of the main lithologies in the region: ultramafic rock (serpentinite, talc-magnesite, talc-chlorite-rich contact zone rocks, $N=40$), phyllite ($N=34$), and greenstone ($N=33$). In the field, the serpentinites are generally massive and knobby to slabby in outcrop with buff-colored 1–3 cm thick weathering rinds; the talc-magnesites tend to be more deeply weathered, often to the point that the outer

10–20 cm is friable. The phyllites, which were sampled from the Hazens Notch, Ottaquechee, Stowe and Moretown formations, often display relict thin-bedded sedimentary layering as well as foliation and are largely unweathered in the field. The greenstones are mainly from metamorphosed mafic igneous bodies within the Stowe Formation; they occur in the field as rounded outcrops with weak foliation and thin buff-colored weathering rinds.

Thin sections were analyzed using optical microscopy and by scanning electron microscopy with an energy dispersive X-ray spectrometer (SEM–EDX) in a Zeiss DSM 940 instrument. Whole-rock geochemistry of the bedrock samples was determined by inductively coupled plasma atomic emission spectrometry (ICP–AES) with a Thermo–Jarrell Ash Iris 1000 instrument at Middlebury College and also by ICP–mass spectrometry (ICP–MS) at Acme Analytical Laboratories in Vancouver, British Columbia. In both cases, rock powders were fused with Li metaborate and dissolved in HNO₃ prior to analysis. Analyses of duplicates and rock powder standards (Canadian Geological Survey MRG-1 and US Geological Survey AGV-2) indicate that analytical errors were <5% for all major elements and <10% for trace elements.

3.2. Whole-rock mineralogy

The mineralogy of ultramafic samples and selected phyllites with elevated As was determined by X-ray diffraction (XRD) and Fourier transform infrared (FTIR) analysis (Moen, 2010; Ryan et al., 2010). Powders for XRD analysis were prepared for internal standard-based quantitative mineral analysis as described by Hillier (1999), Śródoń et al. (2001) and Ryan et al. (2008). Five serpentinites, five talc–magnesites and two steatites (talc-dominated rock) were also analyzed using synchrotron-based XRD at beamline 13-BM-C at the Advance Photon Source, Argonne National Laboratory with a MAR 165 CCD camera.

3.3. Targeted chemical extraction of serpentinite and talc–magnesite

In order to examine potential for release of As from fresh rock and also to examine As speciation, a two-step sequential chemical extraction paired with whole-rock geochemical analyses and the XRD/FTIR analyses described above was applied to 11 serpentinite samples. Step 1 exposed 3.0 g of rock powder to a 100 mL solution of 1 M NH₄NO₃ at 20 °C and initial pH = 4.7 followed by a rinse with 100 mL of 1 M NH₄NO₃. This step was designed to extract As and other elements contained in exchange sites. Step 2 was an aqua regia extraction of 1 g of rock powder that had already been extracted by the step 1 NH₄NO₃ extraction. The aqua regia solution consisted of 10 mL of (1:1) HNO₃ and 25 mL of (1:4) HCl and the rock powder was extracted for 30 min at 95 °C. In order to examine As speciation in talc–magnesites, powders of an As-rich sample (*Well C-3m*) and a relatively As-poor sample (*Well B-26m* and a replicate of this same powder) were extracted by a five-step extraction sequence using a series of progressively stronger reagents, as follows: (1) 1 M NH₄NO₃, as above, (2) 0.11 M acetic acid at 20 °C and initial pH = 2.6, (3) 8.5 M HNO₃ at 20 °C, (4) 8.5 M HNO₃ at 50 °C, and (5) aqua regia (as above). For comparison, a talc-rich rock with no magnesite was also extracted by this series of five extractions. The compositions of the extracted solutions were determined by a combination of ICP–AES and ICP–MS as described above for whole-rock analysis.

3.4. Installation of monitoring wells

In order to establish better lithologic control and to more precisely explore the potential for ultramafic-derived As in groundwater, three monitoring wells were drilled and produced in a groundwater recharge area where ultramafic rock forms a

topographic high point (Barnes Hill)—the goal here was to sample waters which had directly infiltrated the ultramafic rocks and had not been affected by interaction with the other bedrock types. The lithologies of the three wells are as follows: Well A consists of 35 m of serpentinite and talc–magnesite rock atop 21 m of greenish-gray phyllite of the Stowe Formation. The boundary between ultramafics and underlying phyllite is a thrust fault. Well B produces entirely from serpentinite and talc–magnesite rock above the thrust fault. Well C consists of 6 m of talc–magnesite atop gray–black phyllite of the Ottaquechee Formation. Again, the contact is a thrust fault. A thin (1–2 m) layer of glacial till covers the bedrock and mineralogical and geochemical analysis indicates that the till contains a mix of ultramafic and phyllite clasts (Chow, 2009).

Wells were constructed according to standard methods (USEPA, SESDGUID-101-R0, “Design and Installation of Monitoring Wells”, 2008)—details of well construction and data analysis are presented in Chow (2009). Groundwater was produced using peristaltic or bladder pumps and water was sampled after 30 min of pumping. Samples were collected in acid-washed, HDPE bottles and stored on ice for delivery to analytical laboratories. Temperature, conductivity, pH, Eh, and % dissolved O₂ (DO) data were collected in the field using a YSI multiprobe.

3.5. Chemical analysis of groundwaters

Groundwaters were analyzed for concentrations of metals, metalloids and anions at the Vermont Department of Environmental Conservation Laboratory in Waterbury. Samples were acidified and filtered (digested) before analysis. Metals and metalloids were determined by ICP–MS according to USEPA method 6020. Arsenic detection limit is 1 µg/L (13 nm/L) and speciation was not determined. Anions were determined by a combination of ion chromatography (US EPA method 300.0) and other methods (e.g. flow-injection colorimetry) as follows: SM4500-PH (P), SM4500-SiO₂ F (SiO₂) and SM2320-B (alkalinity). Precision and accuracy of analyses were within ±10% (and commonly within 5%) based on replicate analyses and comparison to standards.

4. Results

4.1. Geochemistry of bedrock aquifer lithologies

Average values for the whole-rock geochemistry of ultramafic rocks (separated into subcategories of serpentinite, talc–magnesite and contact zone rocks that are rich in talc or chlorite), meta-sedimentary rocks and metavolcanic rocks are presented in Table 1. Data on the detailed mineralogy and geochemistry of the ultramafic rocks are presented in Table 2.

Whole-rock major element values of serpentinites and talc–magnesites analyzed are generally typical of altered ultramafic rocks. The majority of serpentinites contain, on a wt.% basis (anhydrous), 39–43% MgO, 42–49% SiO₂, 9–14% Fe₂O₃, 1.1–3.1% Al₂O₃, and <1% each of CaO, Na₂O and K₂O (Tables 1 and 2). Regarding trace elements, Cr and Ni values are mainly in the range of 1500–2500 ppm, and others such as Cu, Pb, Zn and Ti are <100 ppm. Notably anomalous is As, which occurs in concentrations from 19 to 449 ppm in serpentinite (mean = 87 ppm). The talc–magnesites are generally more Mg-rich and Si-poor than the serpentinites, with 40–56% MgO and 31–48% SiO₂. The other major and trace elements are similar in concentration to the serpentinites, including As, which is highly variable and extremely elevated in a few samples—the range of As in the talc–magnesite rock is 1–1105 ppm, and while the mean of the 17 talc–carbonates analyzed is 92 ppm As, the median is only 5 ppm As. Talc-rich ultramafic rock (steatite) and chlorite-rich ultramafic rock, which

Table 1
Summary of the whole-rock geochemistry of ultramafic, meta-sedimentary and metabasaltic rocks in the study area. Values represent means and, in italics, range of values.

Lithology	Major element geochemistry (wt.%)							Trace elements (ppm)				
	SiO ₂	Al ₂ O ₃	Fe ₂ O ₃	MgO	CaO	Na ₂ O	K ₂ O	As	Cr	Ni	Cu	Zn
Serpentinite mean	45.9	2.2	9.1	40.4	1.2	0.8	0.2	87	1912	1766	16	63
Range (N = 16)	42.9–49.0	0.6–11.2	7.4–14.5	21.1–43.7	0.2–3.7	<4.0	<2.6	19–449	685–2640	709–2540	8–28	32–183
Talc–magnesite mean	38.2	0.90	10.0	48.1	0.90	0.01	0.01	92	2608	1641	3.4	6.6
Range (N = 17)	31.1–47.8	0.6–1.3	7.4–13.2	40.1–56.2	0.2–2.8	≤0.05	≤0.05	1.0–1105	1676–4400	1373–1990	≤7	≤10
Talc–chlorite mean	53.4	8.9	10.0	20.2	5.3	0.4	0.2	106	2020	1693	28	61
Range (N = 7)	32.9–58.5	1.0–23.6	4.6–23.5	11.6–29.7	0.5–11.3	≤2.1	≤1.3	51–189	1620–2380	1340–2280	8–100	31–109
Meta-sedimentary mean	61.4	17.3	8.0	2.9	2.0	3.1	5.0	22	87	80	50	74
Range (N = 34)	50.7–81.2	4.6–28.6	0.9–15.8	0.4–7.8	0.2–13.3	0.3–6.8	0.03–10.3	<1–190	15–340	11–110	6–100	11–219
Metabasaltic mean	47.0	14.8	12.4	7.0	11.8	2.6	0.3	4	247	**	70	44
Range (N = 33)	42.7–50.7	13.4–16.7	9.6–17.0	4.8–9.3	7.9–16.3	1.0–4.3	≤1.0	<1–69	21–547		16–140	6–102

The talc–chlorite rocks occur at the outer margin of ultramafic bodies near the contact with meta-sedimentary rock. The talc-rich rock is often referred to as steatite. The meta-sedimentary rocks analyzed herein are mainly phyllites although some samples contain layers of quartzite or lenses of carbonate. Whole-rock Ni data are unavailable for the metavolcanic rocks. Data from similar rocks in the region indicates whole-rock Ni is generally 50–200 ppm (Kim et al., 2003). Additional sources of data include Anderson (2006), Bright (2006), Morris (2006), Sullivan (2007) and Chow (2009).

occur locally at the contact between ultramafic bodies and phyllite, are also elevated in As, with concentrations ranging from 51 to 189 ppm As (mean = 106 ppm). Their major element concentrations are more varied than the serpentinites and talc–carbonates, likely reflecting influx of Al, Ca, K and Na from meta-sedimentary rock, paired with loss of Mg to the surrounding meta-sedimentary rock (Cady et al., 1963).

Compositions of phyllites and greenstones are typical for low-grade meta-sedimentary (Hurowitz and McLennan, 2005) and metabasaltic rocks (e.g. Floyd and Winchester, 1978; Kim et al., 2003) from the northern Appalachians. Compared to the ultramafic rocks, the phyllites are enriched in SiO₂, TiO₂, Al₂O₃, Na₂O and K₂O and depleted in MgO, As, Cr and Ni (Anderson, 2006). Greenstones are enriched in Al₂O₃, Fe₂O₃, CaO and Na₂O and depleted in MgO, As, Cr and Ni (Morris, 2006) relative to the ultramafic rocks (Table 1).

The most striking feature of the geochemistry of the bedrock from the RHB is the elevated concentrations of As in ultramafic rocks, both in terms of absolute concentrations and also in terms of their contrast to the other main rock types in the study area (Bright, 2006; Sullivan, 2007; Chow, 2009). Data from 40 ultramafic rock specimens sampled from outcrops and well cuttings reveal a mean As value for all ultramafic rocks of 93 ppm and a range of 1–1105 ppm. For reference, crustal average is approximately 2 ppm (Taylor and McLennan, 1995). Of the 40 ultramafic rock samples, 26 contain As in excess of 20 ppm. By contrast, metabasalt greenstones (N = 33) contain a mean As concentration of 4.1 ppm, and only two contain greater than 20 ppm As; all of the remaining greenstones contain <2 ppm As. Meta-sedimentary rocks (mainly phyllites) contain an average As concentration of 22 ppm (N = 34 samples), a value that includes isolated high concentrations (33–190 ppm) from well cuttings from an interval below a thrust slice of As-rich talc–magnesite—these meta-sedimentary specimens contain detectable talc and magnesite (by XRD), suggesting introduction of ultramafic particles into these samples by the drilling process, or infiltration of water in the fractured aquifer, or tectonically-related insertion of ultramafic fault slivers. Only 10 of the 34 phyllites contain As in excess of 20 ppm and seven of those are well cuttings sampled from the interval below the above-mentioned overthrust As-rich talc–magnesite. If these seven ultramafic-affected samples are removed from the phyllite suite, average phyllite As concentration is 8.0 ppm.

4.2. Mineralogy of bedrock aquifer lithologies

4.2.1. Serpentinities

Whole-rock mineralogical analysis by internal standard-based XRD indicates that the serpentinites sampled for this study contain 78–99% (by wt.) antigorite, with an average value of 92% (Table 2).

Spinel group minerals (chromite + magnetite) comprise <2–7% of serpentinites, carbonates occur locally (up to 5% of whole-rock), and alkali feldspars (3–15%) occur in serpentinites near a fault zone. These data are consistent with mineralogical analyses from Cady et al. (1963), Labotka and Albee (1979) and Levitan et al. (2009). Optical microscopy paired with SEM–EDX analyses did not reveal any sulfides or arsenides and all opaque minerals were identified as spinel-group magnetites or chromites. Sulfides were also not detected by XRD, and geochemical analysis indicates that S comprises <100 ppm of all but four of the ultramafic rocks (four samples contain between 100 and 500 ppm S), and in these four samples, S exhibits no correlation with As. Labotka and Albee (1979) provide no evidence for sulfides in the specimens they analyzed from this region; however, Levitan et al. (2009) found trace amounts of heazlewoodite (Ni₃S₂) in serpentinites from the Belvidere ultramafic (central part of the study area) but no arsenides or As-bearing sulfides. In a sample from an ultramafic locality near Belvidere Mountain in northern Vermont, Chidester et al. (1978) observed a white opaque mineral that they suggested might be gersdorffite (NiAsS); however, while Levitan et al. (2008) report 3–63 ppm As in antigorite-dominated serpentinites from the same study area, they do not present any evidence for As-bearing sulfides or arsenides.

XRD analyses (Fig. 2) indicate that the serpentinites are dominated by poorly ordered antigorite. Substitution of Al for Si in the tetrahedral sheet of antigorite is indicated by d(001) values that range from 7.26 to 7.28 Å (where progressive substitution of Al for Si decreases d(001) of antigorite to values ≤7.30 Å; Serna et al., 1979). Evidence from FTIR analyses (e.g. Al–O stretching vibration at 880–890 cm⁻¹) is also consistent with the occurrence of tetrahedral Al (Ryan et al., 2010), and Levitan et al. (2009) provide electron microprobe data indicating that antigorite crystals from the Belvidere ultramafic within the study area contain 0–17% Al₂O₃ (and 0.5–7% Fe₂O₃), values that bracket SEM–EDX analyses of antigorite composition by Bright (2006) on some of the same samples analyzed in this study. The presence of tetrahedral Al has implications for charge balance associated with the occurrence of As in antigorite, as discussed below (Section 5.1).

4.2.2. Talc–magnesites

The talc content of the talc–magnesites ranges from 33% to 74% and magnesite content is 18–47% and varies inversely with respect to talc. Up to 5% dolomite occurs in the talc–magnesites and chromite + magnetite is <2–7% of whole-rock. All opaque minerals in these samples are the above-mentioned spinel-group oxides or poorly ordered Fe-hydroxides and no evidence was observed of sulfides or arsenides. For the majority of samples, As concentration in the talc–magnesites is not related to the presence or abundance

Table 2

Whole-rock mineralogy and geochemistry for ultramafic rocks from northern Vermont. Samples are arranged from interiors of ultramafic bodies (serpentinite) outward towards contacts with meta-sedimentary rocks (where steatite and chlorite generally occur within meters of the contact).

Sample ID	Lithology	Whole-rock mineralogy (wt.%)										Major element geochemistry (wt.%)							Trace elements (ppm)				
		Antig	Talc	Chl	MgCO ₃	CC	Dolo	Spnl	Qtz	Feld	SUM	SiO ₂	Al ₂ O ₃	Fe ₂ O ₃	MgO	CaO	Na ₂ O	K ₂ O	As	Cr	Ni	Cu	Zn
BV-core	Serpentinite	96.6	<3	<3	<1	1.4	<2	<2	<1	<1	98.0	46.1	1.1	8.4	43.2	0.6	<0.01	<0.01	97	2220	1940	28	48
LD-0404	Serpentinite	94.9	<3	<3	<1	2.3	<2	<2	<1	<1	97.2	45.8	1.1	9.0	42.6	1.3	<0.01	<0.01	34	2200	2280	11	32
LD-0410	Serpentinite	92.8	<3	<3	<1	<1	<2	3.0	<1	<1	95.8	45.0	2.3	11.1	41.4	0.3	<0.01	<0.01	43	2040	1810	15	42
LD-0417	Serpentinite	96.0	<3	<3	<1	<1	<2	<2	<1	<1	96.0	46.2	0.6	8.5	43.7	0.3	<0.01	<0.01	27	2380	1980	8	54
BV-2A	Serpentinite	96.9	<3	<3	<1	2.6	<2	<2	<1	<1	99.5	47.5	1.6	7.9	40.5	2.4	<0.01	<0.01	19	2220	1940	28	48
BV-2B	Serpentinite	90.6	<3	<3	3.8	2.7	<2	<2	<1	<1	97.1	44.8	2.3	8.7	41.4	2.5	<0.01	<0.01	49	1940	1870	16	33
BV-2E	Serpentinite	95.7	<3	<3	<1	<1	<2	<2	<1	<1	95.7	46.9	3.1	7.7	41.7	0.4	<0.01	<0.01	26	685	985	11	51
BV-2F	Serpentinite	96.7	<3	<3	<1	<1	<2	<2	<1	<1	96.7	47.4	1.1	8.7	41.8	0.9	<0.01	<0.01	23	870	936	12	64
BV-3	Serpentinite	90.2	<3	<3	<1	3.6	<2	3.6	<1	<1	97.4	42.3	1.4	9.1	43.3	3.7	<0.01	<0.01	198	869	709	10	183
KB BH-1	Serpentinite	98.8	<3	<3	<1	<1	<2	<2	<1	<1	98.8	49.0	1.3	7.4	41.2	0.5	0.4	<0.01	21	2130	2140	17	66
KB BH-2	Serpentinite	98.0	<3	<3	<1	<1	<2	<2	<1	<1	98.0	48.0	1.3	8.6	41.2	0.2	0.4	0.1	35	2630	2540	24	66
KB BH-3Ox	Serpentinite	92.2	<3	<3	4.9	<1	<2	<2	<1	<1	97.1	45.2	1.3	10.1	42.2	0.3	0.7	0.1	36	3240	2050	11	62
KB BH-5	Serpentinite	88.7	<3	<3	<1	<1	<2	7.2	<1	<1	95.9	46.1	2.0	7.4	39.9	0.8	3.5	0.1	106	1830	1880	11	56
KB BH-3G	Serpentinite	89.3	<3	<3	4.2	<1	<2	<2	<1	2.6	96.1	43.4	2.1	14.5	38.6	0.6	0.3	0.2	103	2640	2010	14	64
KB BH-4W	Serpentinite	89.4	<3	<3	<1	1.1	<2	<2	<1	8.6	99.1	42.9	1.6	8.6	42.6	0.9	3.0	0.1	449	1440	2030	10	58
KB BH-4D	Serpentinite	78.3	<3	<3	<1	3.1	<2	<2	<1	15.3	96.7	47.6	11.2	9.7	21.1	2.9	4.0	2.6	194	1250	1150	22	77
Well A-2m	Talc-MgCO ₃	<3	72.5	3.5	18.6	<1	<1	<2	1.2	<2	95.8	47.4	1.2	9.3	40.3	0.1	0.05	0.05	33	2149	1981	6	8
Well A-3m	Talc-MgCO ₃	<3	62.2	<3	31.3	<1	<1	<2	<1	<2	93.5	38.5	0.9	9.3	49.7	0.1	<0.01	<0.01	3	1779	1760	0	5
Well A-9m	Talc-MgCO ₃	<3	62.7	<3	31.7	<1	<1	<2	<1	<2	94.4	38.1	0.9	9.4	49.8	0.2	<0.01	<0.01	4	1847	1730	5	6
Well A-15m	Talc-MgCO ₃	<3	60.2	4.3	31.8	<1	<1	<2	<1	<2	96.3	37.3	0.8	9.5	50.5	0.3	<0.01	<0.01	1	1998	1712	1	5
Well A-20m	Talc-MgCO ₃	<3	63.5	<3	31.0	<1	2.8	<2	<1	<2	97.3	39.5	0.9	9.4	47.3	1.2	<0.01	<0.01	2	2470	1728	4	6
Well A-21.5m	Talc-MgCO ₃	<3	52.4	<3	41.3	<1	1.9	<2	<1	<2	95.6	32.4	0.8	11.0	53.2	0.7	<0.01	<0.01	2	2758	1582	3	6
Well A-27.5m	Talc-MgCO ₃	<3	54.0	<3	39.1	<1	3	<2	<1	<2	96.1	31.1	0.6	10.2	55.1	1.4	<0.01	<0.01	9	1676	1460	3	6
Well A-32m	Talc-MgCO ₃	<3	58.4	<3	36.6	<1	<1	<2	<1	<2	95.0	33.8	0.8	10.8	52.4	0.4	<0.01	<0.01	9	3086	1590	2	7
Well B-1.5m	Talc-MgCO ₃	<3	62.2	5.1	26.9	<1	<1	<2	1.7	<2	95.9	41.7	1.3	9.5	45.6	0.2	0.03	<0.01	4	2313	1848	3	7
Well B-6m	Talc-MgCO ₃	<3	52.7	<3	36.2	<1	1.9	4.0	<1	<2	94.8	33.7	1.2	10.7	52.0	0.8	<0.01	<0.01	2	2244	1551	1	6
Well B-7.5m	Talc-MgCO ₃	<3	65.1	<3	29.0	<1	1.4	<2	<1	<2	95.5	40.8	1.0	9.6	46.0	0.6	<0.01	<0.01	7	3770	1990	6	8
Well B-13.5m	Talc-MgCO ₃	<3	40.3	3.8	46.6	<1	2.2	6.7	<1	<2	99.6	26.6	0.7	13.2	56.2	1.2	<0.01	<0.01	5	3579	1456	3	8
Well B-20m	Talc-MgCO ₃	<3	49.6	<3	45.5	<1	2.1	2.2	<1	<2	99.4	32.0	0.8	11.5	52.6	1.1	<0.01	<0.01	5	3531	1373	2	6
Well B-26m	Talc-MgCO ₃	<3	60.8	<3	30.1	<1	2.4	6.3	<1	<2	99.6	39.2	1.1	12.0	44.3	1.3	<0.01	<0.01	23	4400	1582	3	10
Well B-26m-u	Talc-MgCO ₃	<3	74.4	<3	17.8	<1	3.3	<2	<1	<2	95.5	47.8	1.0	7.4	40.3	2.0	<0.01	<0.01	19	1882	1795	3	6
Well C-1.5m	Talc-MgCO ₃	<3	34.0	<3	36.8	<1	4.0	<2	19.8	<2	94.6	43.6	1.1	9.0	42.1	2.8	<0.01	<0.01	341	2655	1172	7	6
Well C-3m	Talc-MgCO ₃	<3	32.7	4.6	31.2	<1	2.7	<2	24.5	<2	95.7	46.8	1.3	9.0	40.1	1.3	0.03	<0.01	1105	2196	1582	6	7
121306-6	Steatite	<3	84.8	<3	<2	<1	11.2	<2	<1	<2	96.0	54.7	1.0	4.6	26.6	10.1	0.1	<0.01	142	2200	2280	11	32
121306-5	Steatite	<3	86.8	<3	<2	<1	9.0	<2	<1	<2	95.8	55.1	1.9	6.6	27.2	8.7	0.3	<0.01	84	1840	1340	16	37
121306-4B	Steatite	<3	93.3	<3	<2	<1	3.6	<2	<1	<2	96.9	58.5	1.0	6.5	29.7	2.8	<0.01	<0.01	70	2350	1510	100	109
121306-4	Steatite	<3	86.4	<3	<2	<1	12.6	<2	<1	<2	99.0	56.1	4.1	6.0	21.9	11.3	0.2	<0.01	51	2380	1980	8	54
121306-3	Talc-chlorite	<3	71.7	22.3	<2	<1	<1	<2	<1	<2	94.0	58.0	14.4	13.7	12.2	0.5	0.1	<0.01	82	1620	1520	30	36
121306-2	Talc-chlorite	<3	74.1	21.8	<2	<1	<1	<2	<1	<2	95.9	58.5	16.4	9.0	11.9	0.8	2.1	0.3	189	1810	1350	13	79
121306-1B	Chl margin	<3	<3	62.0	<2	<1	<1	12.5	10.0	8.4	92.9	32.9	23.6	23.5	11.6	3.1	0.2	1.3	126	1940	1870	15	78

Talc-MgCO₃ = talc-magnesite; Chl = chlorite; Antig = antigorite; CC = calcite; Dolo = dolomite; Spnl = magnetite + chromite; Qtz = quartz; Feld = alkali feldspar.

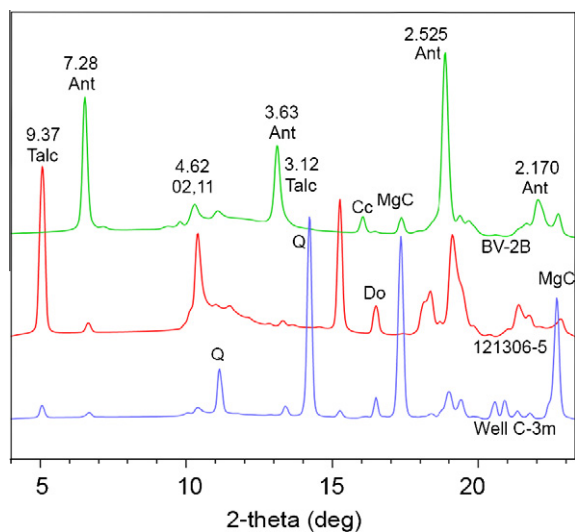


Fig. 2. Synchrotron XRD patterns of representative ultramafic rocks. BV-2B is representative of serpentinites consisting mostly of antigorite (Ant); this particular sample also contains magnesite (MgC) and calcite (Cc). 121306-5 is steatite composed primarily of talc with lesser dolomite (Do). Well C-3m is a talc–magnesite–quartz (Q) rock. The X-ray wavelength is 0.82841 Å and d-spacings are indicated in Å above peaks.

of any particular trace mineral and seems to vary independently of mineral assemblage. The two notable exceptions are the samples from the upper part of monitoring well C, *Well C-1.5m* and *Well C-3m*, which contain 341 and 1105 ppm As, respectively. These are the only two talc–magnesites that contain quartz (19.8% and 24.5%, respectively)—these types of talc–magnesite–quartz rocks occur irregularly in small bodies within talc–magnesite, often in association with fault contacts or shear zones, and likely are produced by metamorphism and metasomatism in the presence of Si-bearing fluids (Chidester et al., 1978). The As-rich sample *Well C-1.5m* is from the chemically-weathered saprolitic zone 1.5 m below the contact of soil and saprolite and contains approximately 5% Fe-hydroxide that appears to be forming via dissolution of magnesite (based on observations of well cuttings) but the Fe-hydroxide is too disordered to be precisely quantified by XRD. *Well C-3m* is largely unweathered. In unweathered samples of this rock type, the talc, magnesite and quartz all occur as individual 0.2–2 mm grains; the talc grains are blocky, magnesite grains are anhedral to rhombohedral, and the quartz is largely anhedral. As the magnesite weathers out, the texture of the rock becomes similar to poorly-consolidated sand.

4.2.3. Steatite, talc–chlorite and chlorite rock

Rocks dominated by talc or chlorite or mixtures of the two occur in the outer fringes of ultramafic bodies near fault-bounded contacts with meta-sedimentary rocks. Steatites contain 85–93% talc and 3–13% dolomite and non-detectable amounts of other minerals. Two talc–chlorite rocks contain ~70% talc and 22% chlorite, and one sample of a contact zone rock contains 62% chlorite and approximately 12% spinel (chromite + magnetite), 10% quartz and 8% plagioclase feldspar. Arsenic concentrations of these rocks range from 51 to 189 ppm and do not exhibit correlations with any detected minerals. Sequential chemical extraction analyses indicate that the As in these samples is contained in talc, chlorite or magnetite (Moen, 2010).

4.3. Sequential chemical extraction of serpentinites

The mildly acidic NH_4NO_3 solution (pH = 4.7) extracted detectable As from two samples, *KB BH-4W* and *KB BH-4D*, which are the

two most As-rich serpentinites in the sample suite (449 ppm and 194 ppm As in whole-rock, respectively) (Table 3).

Neither *KB BH-4W* nor *KB BH-4D* produced detectable S (<500 mg/kg) during NH_4NO_3 extraction, suggesting sulfides are not the As source. The concentrations of Mg and As released into solution during aqua regia extraction (Fig. 3) are positively correlated with the exception of two outliers (two of three late-stage fibrous antigorites), indicating in nearly all samples that the As is affiliated with antigorite and that it is released to solution when antigorite dissolves. The dissolution of antigorite during aqua regia extraction is confirmed by XRD as well as stoichiometric calculations of extracted solutions, and with the exception of BV-2B, which contains 3.8% magnesite, the only known Mg-bearing mineral in these samples is antigorite. Nickel, which in serpentinites is known to occur primarily in the octahedral sheet of antigorite or other serpentine polytypes (Caillaud et al., 2009), is also positively correlated with antigorite dissolution.

4.4. Sequential chemical extraction of talc–magnesites

Extraction of As from talc–magnesite rocks is proportional to the extent of magnesite dissolution (Fig. 4), strongly suggesting that magnesite hosts As (Moen, 2010). However, given that magnesite only accounts for 65–80% of total As in these samples, it is likely that As also occurs in magnetite (Niu et al., 2010) or talc, or both. There is no evidence that these more-resistant minerals dissolved during the sequential extraction, behavior that is probably due to buffering of the solutions by carbonate dissolution, a phenomenon that has been observed elsewhere for carbonate-rich powders (Sulkowski and Hirner, 2006). Thus, it is felt that As liberated to solution during these extractions was released by progressive dissolution of magnesite (which was verified by XRD and FTIR; Moen, 2010), and the residual As that remains in post-aqua regia powders is contained in magnetite or talc.

4.5. Hydrochemistry of monitoring wells

Table 4 presents average values from four sampling rounds over a 6-month period (October 2008–March 2009) for three monitoring wells drilled into (and in two cases, through) ultramafic rock (Fig. 5).

The wells are located at a topographic high point which serves as groundwater recharge area, meaning that values in these wells should only reflect the dissolution of bedrock from which they produce.

These wells produce As that is elevated above background (range of values = 1.7–9.4 $\mu\text{g/L}$; mean values = 2.2–6.4 $\mu\text{g/L}$) and exhibit a Mg– HCO_3 hydrochemical signature (Fig. 6) that is typical of weathered serpentinite (Barnes and O’Neil, 1969; Drever, 1997). This ultramafic signature stands in contrast to the Na–K–Cl trending signature of regional phyllite-dominated groundwater west of the study area in a region with no ultramafic rock (Kim et al., 2009).

5. Discussion

The general spatial association of groundwater As and ultramafic rock outcrops in the Rowe–Hawley Belt of north-central Vermont suggests that ultramafic rock is a source of As in this complexly-folded bedrock aquifer system. Nearly all wells with As >10 $\mu\text{g/L}$ occur within 5 km of ultramafic outcrops, and with one exception, all others are within 10 km—the exception is the well located at ~44.6°N, 72.5°W, and this is the only well in the Rowe–Hawley Belt that seems to have no spatial relationship with ultramafics. In some cases, wells that are 5–10 km away from

Table 3
Summary of results of chemical extractions of serpentinites for three representative and illustrative elements. The five columns per element represent (1) mg of the element extracted by sodium acetate (NaOAc) per kg of rock, (2) percentage of the element extracted by NaOAc relative to total amount of the element in the whole-rock, (3) amount of the element extracted by aqua regia (AqReg) expressed as a wt.% (for Mg) and mg/kg (ppm) for As and Ni, (4) percentage of element extracted by aqua regia relative to total amount of the element, and (5) whole-rock (WR) concentration of the element expressed as wt.%.

Sample ID	Texture	Magnesium			Arsenic			Nickel				
		NaOAc (mg/kg)	NaOAc (% of total Mg)	WR (wt.%)	NaOAc (mg/kg)	NaOAc (% of total As)	WR (mg/kg)	NaOAc (mg/kg)	NaOAc (% of total Ni)	WR (mg/kg)		
BV-core	Massive	1942	0.74	9.3	<1	ND	24.7	25.5	5.2	1283	66.1	1940
LD 0404	Massive	13,334	5.1	11.1	<1	ND	9.2	27.1	16.0	1457	63.9	2280
LD 0410	Massive	5022	2.0	10.8	<1	ND	22.4	52.1	16.0	1241	68.6	1810
LD 0417	Massive	3099	1.2	10.4	<1	ND	11.3	41.9	7.5	1204	60.8	1980
BV-2A	Fibrous	2605	1.1	20.0	<1	ND	3.2	33.5	3.3	1184	61.1	1940
BV-2B	Fibrous	1574	0.63	17.3	<1	ND	0.8	3.3	1.5	1292	69.1	1870
BV-2E	Massive	680	0.27	3.8	<1	ND	1.6	12.4	22.5	336	34.1	985
BV-2F	Fibrous	2258	0.90	5.9	<1	ND	2.7	25.2	5.5	419	44.8	936
KB BH-1	Massive	5292	2.1	12.3	<1	ND	10.9	51.9	<05	1424	66.6	2140
KB BH-4W	Massive	24,017	9.3	18.5	13.5	3.0	327	72.8	14.1	1489	73.3	2030
KB BH-4D	Massive	13,117	10.3	10.5	4.5	2.3	152	78.6	11.4	929	80.8	1150

ultramafic outcrops are surficial wells located in glacial deposits derived in part from ultramafic rocks; this is the case with at least three of the wells that occur to the east of ultramafic bodies in the northernmost part of Vermont near the Canadian border (Corenthal, 2010). However, given the rural nature of this region, statistical analysis of this spatial relationship is prohibited by an insufficient number of wells.

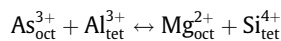
Whole-rock geochemical data indicate that the ultramafic rocks contain a significantly higher concentration of As (mean = 87–106 ppm, depending on rock type) than the other lithologies in the region (mean = 4 and 22 ppm for greenstones and phyllites, respectively), and monitoring wells producing from ultramafic rock show evidence of As derived from dissolution of antigorite and magnesite. Each monitoring well penetrated 1–2 m of saprolitic serpentinite and talc–magnesite beneath glacial till, indicating that these rocks are prone to dissolution in the presence of meteoric water. So, the combination of (1) high As in ultramafic rock, (2) field-based evidence of antigorite and magnesite dissolution, and (3) 2–9 µg/L As in wells producing from fractured ultramafic rock in a low residence time recharge zone are strong evidence that serpentinites and talc–magnesites are As sources in groundwater of this region.

5.1. Speciation of As in ultramafic rocks

Evidence for As in antigorite is provided by chemical extraction data that document positive correlation of As release with antigorite dissolution (Fig. 3), and also by process of elimination given the mineralogical simplicity of these rocks. In many serpentinites, the only two minerals are antigorite and the spinel-group oxides magnetite and chromite. The serpentinite *KB BH-5*, for example, only contains antigorite and spinel-group oxides (based on XRD, FTIR and SEM analysis), so the 105 ppm As in this rock must be contained in the silicate (antigorite) or oxides (magnetite or chromite). Hattori et al. (2005) documented the presence of As in both antigorite and magnetite (but none in chromite) from Himalayan serpentinites using X-ray absorption near-edge structure (XANES), extended X-ray absorption fine structure (EXAFS) and electron microprobe (EMP) analyses. Preliminary XANES, EXAFS and EMP analyses of *KB BH-4* indicates that the As is As³⁺ and that it occurs in antigorite and magnetite (Niu et al., 2010).

The similarity in ionic charges and radii of As³⁺ and Mg²⁺ (Fig. 7) suggests that As can substitute into the octahedral sheet of antigorite and charge balance can be maintained by paired substitution of Al³⁺ for Si⁴⁺ (Fig. 7), the occurrence of which is indicated by antigorite XRD data (Fig. 2) and FTIR data (Ryan et al., 2010).

Given preliminary data from XANES, EXAFS and EMP indicating the presence of As³⁺ in antigorite (Niu et al., 2010) and the indication of tetrahedral Al in site of antigorite from XRD and FTIR (and SEM-EDS; Levitan et al., 2008), the likely scenario involves paired substitution as follows:



Given that numerous substitutions occur in tetrahedral and octahedral sites of antigorites, micas, chlorites and other phyllosilicates (Newman, 1987), it is not surprising that As can occur in either tetrahedral or octahedral sites of antigorite (Hattori et al., 2005). Other recent X-ray absorption studies indicate that As occurs in tetrahedral sites in andradite garnet (Charnock et al., 2007) and tetrahedral or octahedral sites in Mg–smectite (Pascua et al., 2005).

The presence of As in magnetite (Fe₃O₄) has been demonstrated by Hattori et al. (2005), who found up to 60 ppm As in magnetite, and Wang et al. (2008), who indicate that As can be incorporated into magnetite by sorption of As(III) onto the surfaces of magnetite crystals. In a sample from northern Vermont (*KB BH-5*), Niu et al.

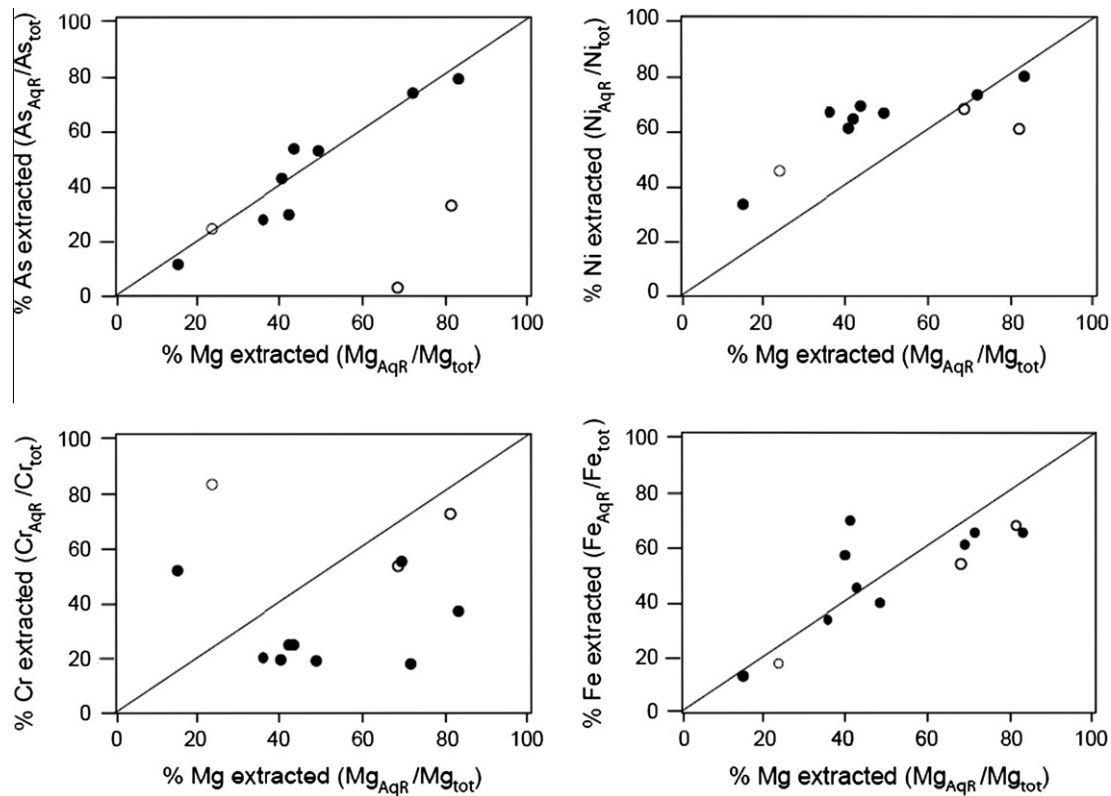


Fig. 3. Bivariate diagrams of elements extracted from serpentine by aqua regia extraction following removal of carbonates and exchangeable cations, Mg, Ni, and Fe occur in the octahedral sheet of serpentine, and the positive correlation of As and Mg in all but two specimens (both later-stage asbestiform serpentine, empty symbols) is consistent with occurrence of As in serpentine octahedral sheets. Scatter in Cr values likely reflects its presence in iron oxides or hydroxides.

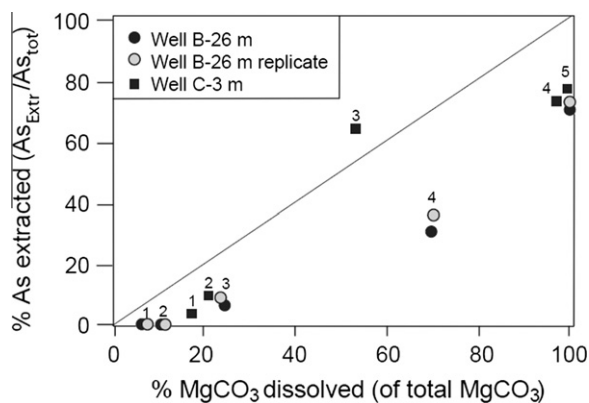


Fig. 4. Bivariate diagram of arsenic extracted as a function of magnesite dissolution from two talc–magnesite rocks is consistent with occurrence of arsenic in magnesite. Extraction steps range from 1 M NH₄NO₃ (ion exchange, step 1) to progressively stronger acids, culminating with aqua regia (step 5). The fact that not all As is released during these extractions implies that some As likely also occurs in magnetite or talc.

(2010) documented the presence of As in magnetite by EMP analysis; however, given low abundances of magnetite in the rocks studied herein (<2%), As concentrations would need to be $\sim 10^4$ – 10^5 ppm in magnetite to produce whole-rock As concentrations on the order of 10^2 – 10^3 ppm. Furthermore, magnetite appears to be very stable in the weathering environment and those analyzed herein show no evidence for dissolution, so the likelihood that As in groundwater is derived from magnetite is low, and magnesite (MgCO₃) or antigorite are more probable sources of groundwater As.

The anomalously high concentration of As in a small proportion of talc–magnesites (e.g. 341 and 1105 ppm) combined with the high reactivity of magnesite in the weathering environment indicates that localized As-rich talc–magnesites may be an important source of As to groundwater. The occurrence of As in magnesite is indicated by sequential chemical extractions (Fig. 4; Moen, 2010); field-based observations indicate that chemical weathering of Fe-bearing magnesite results in incorporation of As into Fe-hydroxides—the Fe-hydroxides form in situ when Mg and CO₃ are leached from the rock (Corenthal, 2010). Thus, the presence of As in magnesite combined with the high solubility of magnesite in the weathering environment may be an important control on release of As. Once released from magnesite, As may be sorbed to secondary Fe-hydroxides as observed by Corenthal (2010) or be liberated as a solute into groundwater. Alexandratos et al. (2007) indicate that AsO₄³⁻ can substitute for carbonate anions in calcite, and given the similarity in structure of magnesite and calcite, it is likely that arsenate anions occur in trace amounts substituted for carbonate anions in magnesite.

Sulfides or arsenides were not detected by analyses of thin sections (by transmitted light microscopy and SEM–EDX) or by XRD, and mass balance calculations from geochemical data help demonstrate that the As in samples with >100 ppm As cannot be derived from sulfide minerals. The most illustrative examples are talc–magnesite sample Well C-3m (1105 ppm As) and serpentinite sample KB BH-4W (449 ppm As), both of which contain <200 ppm S. On a wt.% basis, As is at least 2–5 times more abundant than S in these samples, and on a molar basis, the As:S ratio is at least 1:1 and perhaps much higher given that S is only known to be <200 ppm (for reference, total S is ≤ 51 ppm in serpentinites analyzed by Hattori et al., 2005). There are no known sulfides or sulfarsenides that contain a molar As:S ratio >1, and other than trace amounts of

Table 4

Summary of geochemical data from three groundwater monitoring wells. All three monitoring wells originate in ultramafic rock, and Wells A and C include phyllites below fault zones. All concentrations are ppm except for Fe, As, Cr and Ni, which are ppb. Cond = conductivity (mS/cm); units of Eh are mV.

Sample ID	Lithology	pH	Cond.	Eh	Ca	Ma	SiO ₂	Fe	HCO ₃ ⁻	SO ₄ ²⁻	As	Cr	Ni
Well A	Ultramafic (33.5m) Fault zone (4.5m) Stowe Fm (17m)	7.6	460	+369	8.6	34.5	4.6	280	155	9.2	2.2	6.1	<5
Well B	Ultramafic (27.4m)	7.4	310	+352	16.9	38.2	7.6	284	165	15.0	2.3	5.7	<5
Well C	Ultramafic (4m) Fault zone (3m) Ottaquechee Fm (38m)	7.4	350	+351	16.0	37.4	8.2	580	179	13.7	6.4	<5	<5

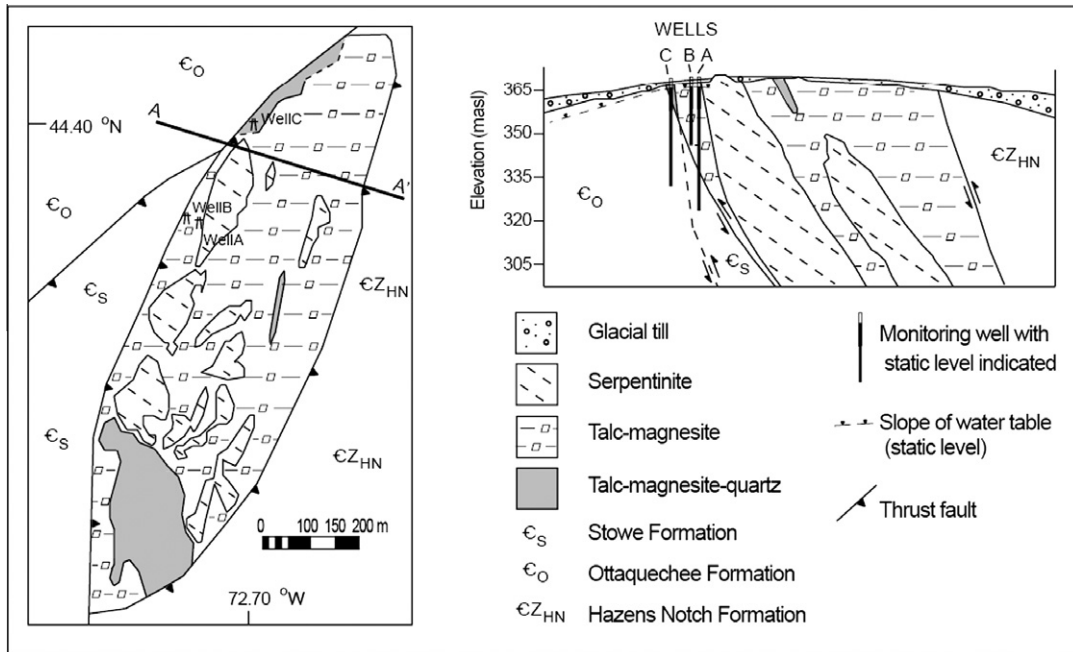


Fig. 5. Geologic map and cross section of bedrock geology and aquifer in location of monitoring wells A, B and C (after Chidester et al., 1952; Chow, 2009). The bedrock samples listed in Table 2 with “KB BH” names are serpentinites from this ultramafic body and the “Well A”, “Well B” and “Well C” samples are well cuttings from the three monitoring wells shown above. Note that the water table slopes from the ultramafic Well B towards both wells A and C. Stowe, Ottaquechee and Hazens Notch formations are phyllites in fault contact with the ultramafic body. Locations of all three wells on the cross section are projected to demonstrate lithologic relationships.

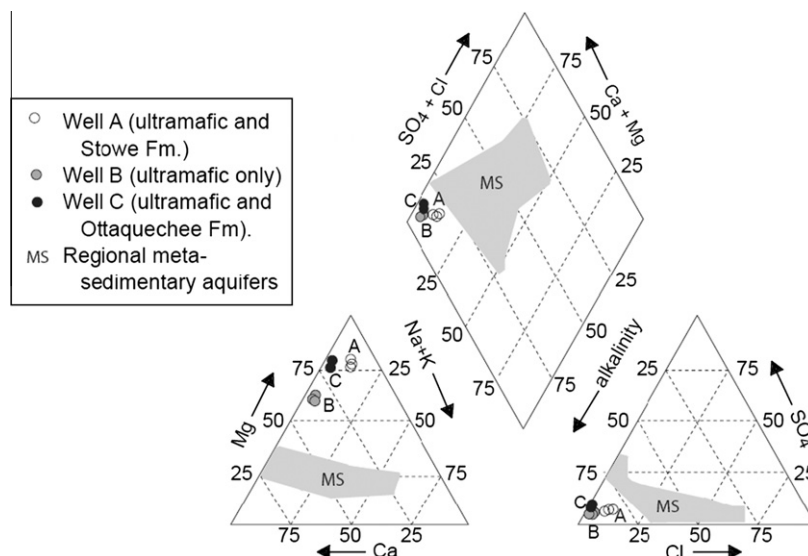


Fig. 6. Piper plots of hydrochemical facies from monitoring wells with ultramafic-dominated signatures (A, B, C) and, for comparison, ground waters derived from meta-sedimentary (phyllite-dominated) rock aquifers in Vermont (Bean, 2009; Kim et al., 2009).

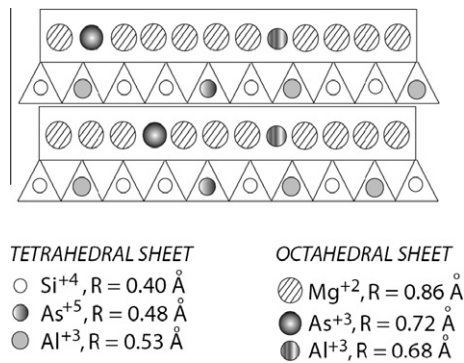


Fig. 7. Schematic sketch of an antigorite crystal depicting substitution of As³⁺ and Al³⁺ for Mg²⁺ in the octahedral sheet, and As⁵⁺ and Al³⁺ for Si⁴⁺ in the tetrahedral sheet. Note that paired substitution of As and tetrahedral Al can maintain charge balance regardless of whether As is tetrahedral or octahedral. Ionic radii (R) are from Shannon (1976).

an opaque white mineral that was not positively-identified but may have been gersdorffite (NiAsS; Chidester et al., 1978), neither As sulfides (e.g. realgar, AsS and orpiment, As₂S₃) nor sulfarsenides (e.g. arsenopyrite) or arsenides (e.g. niccolite) have been observed in Vermont ultramafic rocks, either in this study or in previous ones (e.g. Cady et al., 1963; Labotka and Albee, 1979; Levitan et al., 2009). The presence of authigenic magnetite attests to conditions that are probably too oxidizing to permit formation of sulfides and arsenides. Furthermore, the most common As-bearing sulfide mineral in groundwater systems is arsenian pyrite (Nordstrom, 2002; Smedley and Kinniburgh, 2002; Peters and Burkert, 2008), and even using an anomalously high value for As content in pyrite (77,000 ppm; Smedley and Kinniburgh, 2002), it is clear that there is far too little S in these rocks to indicate an arsenian pyrite source of As. Thus, the data are consistent with As derived from silicate, oxide or carbonate sources in these ultramafic rocks.

5.2. Origin of As in the ultramafic rocks

The ultramafic bodies in Vermont are metasomatically-altered peridotites that originated as dunites (and less commonly harzburgites) which were obducted in the suture zone associated with the Ordovician Taconian Orogeny (Stanley and Ratcliffe, 1985; Coish and Gardner, 2004). These bodies were deformed and altered to serpentinite or talc–magnesite under greenschist to lower amphibolite facies conditions during a series of events that likely began during subduction in the early Ordovician and continued periodically until Devonian time (van Baalen et al., 1999; Coish and Gardner, 2004). There is no consensus regarding the specific mechanisms and components of subduction and collision but what is apparent is that subduction was protracted and may have taken place over tens of millions of years, e.g. from 500 to 443 Ma (Stanley and Ratcliffe, 1985; Ratcliffe et al., 1998).

Arsenic is typically depleted in ultramafic rocks relative to other rock types, particularly compared to deep sea clays (and shales and slates) and intermediate to felsic igneous rocks including arc volcanics and pegmatites (Nordstrom, 2002; Smedley and Kinniburgh, 2002; Peters and Blum, 2003). For example, the concentration of As in the anhydrous primitive mantle has been estimated to be 0.05 ppm (McDonough and Sun, 1995) and mean ultramafic As concentration is 1.5 ppm (Smedley and Kinniburgh). Smedley and Kinniburgh (2002) report marine shales and slates with mean whole-rock As concentrations of 3–174 ppm depending on locality; Peters and Blum (2003) document felsic pegmatites in New Hampshire, USA with whole-rock As concentrations an order of magnitude greater than other lithologies in the region and As

values as high as 60 ppm; and Hattori et al. (2005) present a synthesis of volcanic arc rocks with values as high as 40 ppm. However, in the Rowe–Hawley Belt of northern Vermont, As is appreciably enriched in ultramafic rocks relative to regional meta-sedimentary rocks (Table 1) which originated as deep sea clays, and the ultramafics from this region also show considerable enrichment compared to most arc volcanics (Fig. 8). Hattori et al. (2005) have also observed As-rich serpentinites with similar enrichment in As (Fig. 8).

Evidence for metasomatic addition of As to the ultramafics is provided by the positive correlation of As with crustally-derived fluid-mobile elements such as light rare earth elements and Sb (Fig. 9), constituents which are considered to be derived from the subducting slab (Schmidt et al., 2003; Hattori et al., 2005; Ishimaru and Arai, 2008).

The initial introduction of As into the ultramafics could have taken place in the early stages of subduction when As-rich fluids were driven off sediments of the subducting slab under greenschist or blueschist metamorphic conditions, an idea that is supported by data from Bebout et al. (1999), who observed progressive loss of As from sediments exposed to prograde metamorphism in subduction zone environments. When undergoing hydration (from olivine to serpentine), ultramafic rocks act as a sponge for metamorphic fluids and there is evidence from various localities that As is incorporated into ultramafic rocks during hydration (e.g. Schmidt et al., 2003; Hattori et al., 2005; Ishimaru and Arai, 2008). The high reactivity of anhydrous ultramafic rocks combined with their potential to incorporate As into silicates and oxides under oxidizing conditions (Hattori et al., 2005), or into sulfides or arsenides under strongly reducing conditions (Ishimaru and Arai, 2008), suggests that when present in environments where As is driven off metasediments, ultramafic rocks are a probable As sink.

Once hydrated to serpentinite, ultramafic bodies become far less reactive (Hattori et al., 2005), and assuming that initial serpentinitization took place in association with subduction prior to the Taconian Orogeny (Coish and Gardner, 2004), it is less likely that the As was introduced to the ultramafic rocks during obduction or after they had been emplaced into the continental crust.

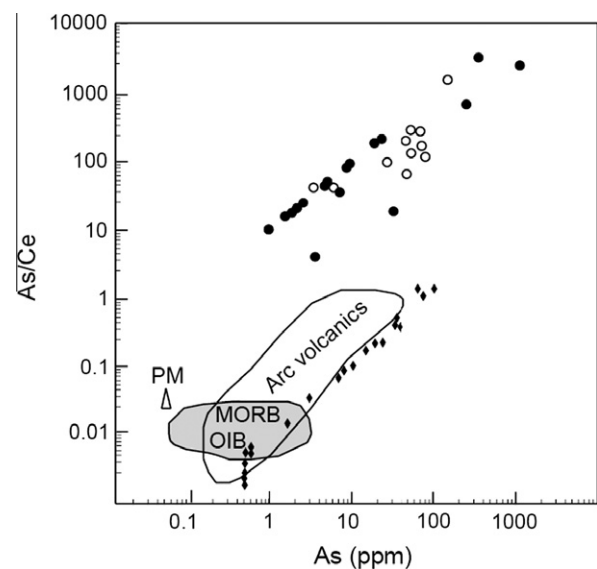


Fig. 8. Bivariate plot of As vs. As/Ce ratio in (1) serpentinites and talc–magnesites from northern Vermont (solid circles), (2) serpentinites from the Himalaya (open circles), arc volcanics, mid-ocean ridge basalts (MORB) and oceanic island basalts (from Hattori et al., 2005 and sources cited therein), and (3) meta-sedimentary rocks from northern Vermont (diamonds). PM is primitive mantle (McDonough and Sun, 1995).

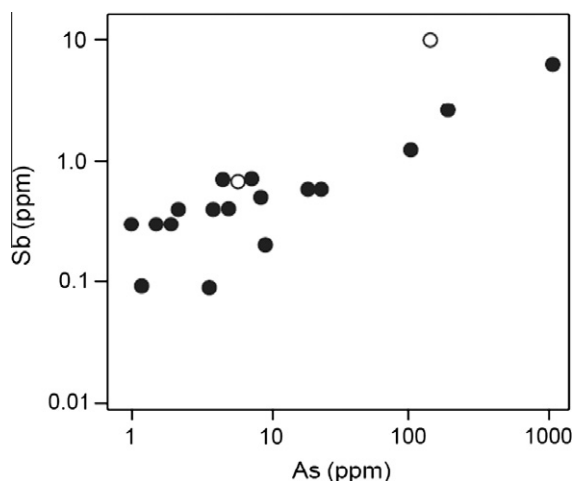


Fig. 9. Bivariate plot of arsenic vs. antimony. Solid circles are serpentinites and talc–magnesites from northern Vermont; open circles are CH 146 and CH 187 from Hattori et al. (2005).

However, evidence of As loss from meta-sedimentary rocks during prograde metamorphism at and above greenschist grade in Maine, USA (O’Shea et al., 2008, 2009) indicates that As is redistributed during regional metamorphism in the continental crust. The meta-sedimentary rocks in the Rowe–Hawley Belt contain, on average, 75–80% less As than the metasomatized ultramafic rocks in this region (Table 1 and Fig. 8), and even sulfide-rich meta-sedimentary rocks in this area are depleted in As relative to the ultramafics, a finding that is similar to results of O’Shea et al. (2008, 2009), who indicated that sulfides in medium- and high-grade metamorphic rocks are depleted in As relative to low-grade rocks. Thus, it is speculated that the majority of As was introduced to the ultramafics during prolonged subduction throughout the Ordovician Period that preceded the arc-continent collision that marked the Taconian Orogeny (Stanley and Ratcliffe, 1985; Coish and Gardner, 2004), but it is also acknowledged that subsequent metamorphic reactions and fluid flow in the continental crust could have also redistributed As, especially in fault zones at the contacts of ultramafic rocks and meta-sedimentary rocks. This process could be responsible for the anomalously high As in the talc–magnesites *Well C-1.5m* and *Well C-3m* (which occur in contact with a shear zone) and also for elevated As in talc-rich and chlorite-rich contact zone rocks.

5.3. Release of As from ultramafic rocks into groundwater

The Mg–HCO₃ hydrochemistry (Fig. 6) of the three bedrock monitoring wells drilled into ultramafics and adjacent meta-sedimentary rocks is typical of groundwaters derived from hydrolysis of serpentinites and related ultramafic rocks (Barnes and O’Neil, 1969). Static levels in the three wells indicate that groundwater flows from the ultramafic-only well B towards the two wells with phyllite at depth (wells B and C). Furthermore, in addition to differentiating ultramafic-derived groundwater from meta-sedimentary-derived groundwater, the Mg–HCO₃ hydrochemical signature also indicates that the Mg minerals (magnesite or antigorite) in the ultramafic rocks are dissolving in the presence of meteoric water or shallow groundwater. Given that these minerals are the probable As source, dissolution of magnesite or antigorite would release As to solution. The HCO₃-dominated anionic load of these waters may enhance As solubility due to the exchange of HCO₃⁻ for arsenite or arsenate anions on the surfaces of Fe-hydroxides, clays and other surface-reactive particles in the aquifer (Smedley and Kinniburgh, 2002).

The low residence time of water in these wells located in a recharge zone likely produces relatively dilute solute concentrations compared to what would be expected for groundwater with higher residence times, yet in spite of this, As concentrations ranged from 2 to 9 µg/L (Table 4) over the 6-month analysis period described in Chow (2009). What this demonstrates is that even in an area of high groundwater flux rates, groundwater flowing through serpentinite and talc–magnesite is capable of producing As concentrations that are elevated over background values (i.e. 1 µg/L; Wedepohl, 1978), and ultramafic rocks are a probable source of >10 µg/L As in more typical aquifer conditions where residence times are greater.

6. Conclusions

Groundwater in bedrock aquifers in the Rowe–Hawley Belt of northern Vermont contains elevated As that appears to be derived from weathering of ultramafic rocks, particularly serpentinites and talc–magnesites, lithologies which contain far greater concentrations of As than regional meta-sedimentary and metaigneous rocks. The As was likely introduced to the ultramafics during metasomatic reactions in the subduction zone that existed prior to and during the arc-continent collision of the Ordovician Taconian Orogeny, and possibly also during obduction or later regional metamorphism. Hydrolysis of the ultramafics and release of As is evident from saprolitic weathering zones at the interface of bedrock and soil and also from the Mg–HCO₃ hydrochemical signature in monitoring wells producing from fractured bedrock dominated by ultramafic rock. Data from whole-rock geochemistry, chemical extraction analysis, XRD and FTIR analysis strongly suggest that the As is derived from the octahedral sheet of antigorite and likely also from magnesite, and that the As is released when these minerals partially dissolve in the presence of meteoric water. It is also recognized that unanswered questions remain—a systematic study of As in mineral structures by XANES and EXAFS analysis could provide direct measurements of As speciation in aquifer solids, and the speciation of As in this groundwater system is also unknown, so future work should also be designed to address this question. Lastly, given the presence of serpentinites with anomalously high As concentrations in the suture zones of the northern Appalachians (this study) and the Himalaya (Hattori et al., 2005), similar anomalies may occur in geologically-analogous terranes globally.

Acknowledgements

This project was supported by the Lintilhac Foundation, the Vermont Geological Society, the Lake Champlain Research Consortium and Middlebury College. Taylor Smith and Arthur Clark assisted with XRD analyses, and a brief conversation with Gail Lipfert helped to underscore some implications of the hydrochemistry of the monitoring wells. We also thank Jeff Hoffer for guidance during development of monitoring wells and Rick Purchase and the crew from the Johnson Artesian Well branch of Spafford Well Drilling for well installation. Finally, we wish to acknowledge the efforts of two anonymous reviewers and guest editors Prosun Bhattacharya, Alan Fryar and Abhijit Mukherjee.

References

- Acharyya, S.K., Chakraborty, P., Lahiri, S., Raymahashay, B.C., Guha, S., Bhowmik, A., 1999. As poisoning in the Ganges delta. *Nature* 401, 545.
- Alexandratos, V.G., Elzinga, E.J., Reeder, R.J., 2007. Arsenate uptake by calcite: macroscopic and spectroscopic characterization of adsorption and incorporation mechanisms. *Geochim. Cosmochim. Acta* 71, 4172–4187.

- Anderson, C., 2006. Geochemistry of Meta-sedimentary Rocks in the Waterbury-Stowe Area, Central Vermont. Unpublished Bachelors Thesis, Middlebury College, Middlebury, Vermont.
- Arai, Y., Sparks, D.L., Davis, J.A., 2004. Effects of dissolved carbonate on arsenate adsorption and surface speciation at the hematite–water interface. *Environ. Sci. Technol.* 38, 817–824.
- Barnes, I., O'Neil, J.R., 1969. The relationship between fluids in some fresh alpine-type ultramafics and possible modern serpentinization, western United States. *Geol. Soc. Am. Bull.* 80, 1947–1960.
- Bean, J.R., 2009. A Geochemical Analysis of Geologic Controls on Naturally-occurring Radioactivity in Groundwater: Hinesburg, Vermont. Unpublished Bachelors Thesis, Middlebury College, Middlebury, Vermont.
- Bebout, G.E., Ryan, J.G., Leeman, W.P., Bebout, A.E., 1999. Fractionation of trace elements by subduction-zone metamorphism effect of convergent-margin thermal evolution. *Earth Planet Sci. Lett.* 171, 63–81.
- Bright, K.S., 2006. Ultramafic Bedrock Source of Arsenic in Private Wells, Stowe, Vermont. Unpublished Bachelors Thesis, Middlebury College, Middlebury, Vermont.
- Cady, W.M., Albee, A.L., Chidester, A.H., 1963. Bedrock geology and asbestos deposits of the upper Missisquoi Valley and vicinity, Vermont, US. *Geol. Surv. Bull.* 1122B.
- Caillaud, J., Proust, D., Philippe, S., Fontaine, C., Fialin, M., 2009. Trace metals distribution from a serpentinite weathering at the scales of the weathering profile and its related weathering microsystems and clay minerals. *Geoderma* 149, 199–208.
- Charnock, J.M., Polya, D.A., Gault, G., Wogelius, R., 2007. Direct EXAFS evidence for incorporation of As⁵⁺ in the tetrahedral site of natural andraditic garnet. *Am. Mineral.* 92, 1856–1861.
- Chidester, A.H., Albee, A.L., Cady, W.M., 1978. Petrology, Structure and Genesis of the Asbestos Bearing Ultramafic Rocks of the Belvidere Mountain Area in Vermont. *US Geol. Surv. Prof. Paper* 1016.
- Chidester, A.H., Stewart, G.W., Morris, D., 1952. Geologic Map of the Barnes Hill Talc Prospect, Waterbury, Vermont: *US Geol. Surv. Mineral Investigations Field Studies Map* MF-7.
- Chow, D.R., 2009. Evidence for Ultramafic-derived Arsenic in Bedrock Monitoring Wells, North-central Vermont. Unpublished Bachelors Thesis, Middlebury College, Middlebury, Vermont.
- Cloutier, V., Lefebvre, R., Savard, M., Bourque, E., Therrien, R., 2006. Hydrogeochemistry and groundwater origin of the Basses-Laurentides sedimentary rock aquifer system, St. Lawrence Lowlands, Québec, Canada. *Hydrogeol. J.* 14, 573–590.
- Coish, R.A., 1997. Rift and ocean floor volcanism from the late Proterozoic and early Paleozoic of the Vermont Appalachians. In: Sinha, K., Whalen, J. (Eds.), *The Nature of Magmatism in the Appalachians*, vol. 191. *Geol. Soc. America Memoir*, pp. 129–145.
- Coish, R.A., Gardner, P.J., 2004. Suprasubduction zone peridotite in the northern USA Appalachians: evidence from mineral composition. *Mineral. Mag.* 68, 699–708.
- Coish, R.A., Perry, D.A., Anderson, C.D., Bailey, D., 1986. Metavolcanic rocks from the Stowe Formation, Vermont: remnants of ridge and intraplate volcanism in the Iapetus ocean. *Am. J. Sci.* 286, 1–28.
- Corenthal, L., 2010. Arsenic in Glacial Drift Aquifers, North-central Vermont. Unpublished Bachelors Thesis, Middlebury College, Middlebury, Vermont.
- Di Benedetto, F., Costagliola, P., Benvenuti, M., Lattanzi, P., Romanelli, M., Tanelli, G., 2006. Arsenic incorporation in natural calcite lattice: evidence from electron spin echo spectroscopy. *Earth Planet Sci. Lett.* 246, 458–465.
- Doll, C.G., Cady, W.M., Thompson Jr., J.B., Billings, M.P., 1961. Centennial Geologic Map of Vermont. *Vermont Geological Survey, Scale 1:250 000*.
- Doolan, B.L., Gale, M.H., Gale, P.N., Hoar, R.S., 1982. Geology of the Quebec Reentrant: possible constraints from early rifts and the Vermont–Quebec serpentine belt. In: St. Julien, P., Beland, J. (Eds.), *Major Structural Zones and Faults of the Northern Appalachians. Special Paper 7. Geol. Assoc. Canada*, pp. 87–115.
- Drever, J.I., 1997. *The Geochemistry of Natural Waters: Surface and Groundwater Environments*, third ed. Simon and Shuster, Upper Saddle River, New Jersey.
- Fendorf, S., Eick, M.J., Grossl, P., Sparks, D.L., 1997. Arsenate and chromate retention mechanisms on goethite. 1. Surface structure. *Environ. Sci. Technol.* 31, 315–320.
- Floyd, P.A., Winchester, J.A., 1978. Identification and discrimination of altered and metamorphosed volcanic rocks using immobile elements. *Chem. Geol.* 21, 291–306.
- Guillot, S., Charlet, L., 2007. Bengal arsenic, an archive of Himalaya orogeny and paleohydrology. *J. Environ. Sci. Health A* 42, 1785–1794.
- Hattori, K., Takahashi, Y., Guillot, S., Johanson, B., 2005. Occurrence of arsenic (V) in forearc mantle serpentinites based on X-ray absorption spectroscopy study. *Geochim. Cosmochim. Acta* 69, 5585–5596.
- Heinrichs, G., Udluft, P., 1999. Natural arsenic in Triassic rocks: a source of drinking-water contamination in Bavaria, Germany. *Hydrogeol. J.* 7, 468–476.
- Hillier, S., 1999. Use of an air-brush to spray dry specimens for X-ray powder diffraction. *Clay Miner.* 34, 127–135.
- Horton, T.W., Becker, J.A., Craw, D., Koons, P.O., Chamberlain, C.P., 2001. Hydrothermal arsenic enrichment in active mountain belt: Southern Alps, New Zealand. *Chem. Geol.* 177, 323–339.
- Hurowitz, J.A., McLennan, S.M., 2005. Geochemistry of Cambro-Ordovician sedimentary rocks of the Northeastern United States: changes in Sediment Sources at the onset of Taconian Orogenesis. *J. Geol.* 113, 571–587.
- Ishimaru, S., Arai, S., 2008. Arsenide in a metasomatized peridotite xenolith as a constraint on arsenic behavior in the mantle wedge. *Am. Mineral.* 93, 1061–1065.
- Kim, J., Jacobi, R.D., 1996. Geochemistry and tectonic implications of Hawley Formation meta-igneous units; northwestern Massachusetts. *Am. J. Sci.* 296, 1126–1174.
- Kim, J., Coish, R., Evans, M., Dick, G., 2003. Suprasubduction Zone extensional magmatism in Vermont and adjacent Quebec: implications for Early Paleozoic Appalachian Tectonics. *Geol. Soc. Am. Bull.* 115, 1552–1569.
- Kim, J., Ryan, P.C., North, K., Bean, J., Davis, L., 2009. Radionuclides, groundwater geochemistry, and hydrogeology above, below, and through the Hinesburg thrust: NW Vermont. *Geol. Soc. Am. Abstr. Prog.* 41, 21.
- Labotka, T.C., Albee, A.L., 1979. Serpentinization of the Belvidere Mountain ultramafic body, Vermont: mass balance and reaction at the metasomatic front. *Can. Mineral.* 17, 831–845.
- Levitani, D.M., Hammarstrom, J.M., Gunter, M.E., Seal II, R.R., Chou, I.-M., Piatak, N.M., 2008. Mineralogical characterization of tailings at the Vermont Asbestos Group Mine, Belvidere Mountain, Northern Vermont. *Geol. Soc. Am. Abstr. Prog.* 40, 256.
- Levitani, D.M., Hammarstrom, J.M., Gunter, M.E., Seal III, R.R., Chou, I.-M., Piatak, N.M., 2009. Mineralogy of mine waste at the Vermont Asbestos Group mine, Belvidere Mountain, Vermont. *Am. Mineral.* 94, 1063–1066.
- Lipfert, G., Reeve, A.C., Sidle, W.C., Marvinney, R., 2006. Geochemical patterns of arsenic-enriched groundwater in fractured, crystalline bedrock, Northport, Maine, USA. *Appl. Geochem.* 21, 528–545.
- McDonough, W., Sun, S.S., 1995. The composition of the Earth. *Chem. Geol.* 120, 223–253.
- Moen, J.C., 2010. Analysis of Arsenic Speciation in Ultramafic Rocks by Sequential Chemical Extraction: Implications for Metasomatizing Fluids and Modern Aquifer Contamination. Unpublished Bachelors Thesis, Middlebury College, Middlebury, Vermont.
- Morris, N., 2006. The Geochemistry Of Meta-volcanic Rocks from the Southern Worcester Mountain Area, Vermont. Unpublished Bachelors Thesis, Middlebury College, Middlebury, Vermont.
- Mukherjee, A., von Brömssen, M., Scanlon, B.R., Bhattacharya, P., Fryar, A.E., Hasan, M.A., Ahmed, K.M., Jacks, G., Chatterjee, D., Sracek, O., 2008. Hydrogeochemical comparison and effects of overlapping redox zones on groundwater arsenic near the western (Bhagirathi sub-basin, India) and eastern (Meghna sub-basin, Bangladesh) of the Bengal basin. *J. Contam. Hydrol.* 99, 31–48.
- Newman, A.C.D., 1987. *The Chemistry of Clays and Clay Minerals. Mineralogical Society, London.*
- Niu, L., Hattori, K., Takahashi, Y., Ryan, P.C., 2010. The occurrence and speciation of arsenic in serpentinites in northern Vermont, USA. In: *IMA 2010: The 20th General Meeting International Mineralogical Association, Budapest.*
- Nordstrom, D.K., 2002. Worldwide occurrences of arsenic in groundwater. *Science* 296, 2143–2145.
- Nordstrom, D.K., Zheng, Y., 2009. Natural arsenic enrichment: effects of the diagenetic–tectonic–hydrothermal cycle. *Geol. Soc. Am. Abstr. Prog.* 41, 217.
- O'Shea, B., MacLean, A., Brock, P., Yang, Q., Marvinney, R., Zheng, Y., 2009. Arsenic-mineral associations in a fractured crystalline aquifer with elevated groundwater arsenic, Maine USA. *Geol. Soc. Am. Abstr. Prog.* 41, 217.
- O'Shea, B., Yang, Q., MacLean, A., Marvinney, R., Brock, P., Zheng, Y., 2008. Arsenic in fractured bedrock aquifers: the influence of prograde metamorphism on arsenic mineralization in the bedrock. *Geol. Soc. Am. Abstr. Prog.* 40, 473.
- Pascua, C., Charnock, J., Polya, D.A., Sato, T., Yokoyama, S., Minato, M., 2005. Arsenic bearing smectite from the geothermal environment. *Mineral. Mag.* 69, 897–906.
- Peters, S.C., Blum, J.D., 2003. The source and transport of arsenic in a bedrock aquifer, New Hampshire, USA. *Appl. Geochem.* 18, 1773–1787.
- Peters, S.C., Burkert, L., 2008. The occurrence and geochemistry of arsenic in groundwaters of the Newark basin of Pennsylvania. *Appl. Geochem.* 23, 85–98.
- Ratcliffe, N.M., Hames, W.E., Stanley, R.S., 1998. Interpretation of ages of arc magmatism, metamorphism and collisional tectonics in the Taconian Orogen of western New England. *Am. J. Sci.* 298, 791–797.
- Robinson, G.R., Ayotte, J.D., 2006. The influence of geology and land use on arsenic in stream sediments and groundwaters in New England, USA. *Appl. Geochem.* 21, 1482–1497.
- Ryan, P.C., Hillier, S., Wall, A.J., 2008. Stepwise effects of the BCR sequential chemical extraction procedure on dissolution and metal release from common ferromagnesian clay minerals: a combined solution chemistry and X-ray powder diffraction study. *Sci. Total Environ.* 407, 603–614.
- Ryan, P.C., Moen, J.C., Corenthal, L.G., Chow, D.R., Kim, J., 2010. Tetrahedral arsenic (As⁵⁺) in antigorite: geological origin and implications for groundwater quality. In: *SEA-CSSJ-CMS Trilateral Meeting on Clays, Seville Spain, T2-P-25.*
- Schmidt, G., Witt-Eickchen, G., Palme, H., Seck, H., Spettel, B., Kratz, K.-L., 2003. Highly siderophile elements (PGE, Re and Au) in mantle xenoliths from the West Eifel volcanic field (Germany). *Chem. Geol.* 196, 77–105.
- Schroetter, J.-M., Tremblay, A., Bedard, J.H., Villeneuve, M.E., 2006. Syn-collisional basin development in the Appalachian orogen—The Saint-Daniel Mélange, southern Québec, Canada. *Geol. Soc. Am. Bull.* 118, 109–125.
- Seddique, A.A., Masuda, H., Mitamura, M., Shinoda, K., Yamanaka, T., Itai, T., Maruoka, T., Uesugi, K., Ahmed, K.M., Biswas, D.K., 2008. Arsenic release from biotite into a Holocene groundwater aquifer in Bangladesh. *Appl. Geochem.* 23, 2236–2248.
- Serna, C.J., White, J.L., Velde, B.D., 1979. The effect of aluminum on the infrared of 7 Å trioctahedral minerals. *Mineral. Mag.* 43, 141–147.

- Shannon, R.D., 1976. Revised effective ionic radii and systematic studies of interatomic distances in halides and chalcogenides. *Acta Cryst.* A32, 751–767.
- Shilts, W.W., Smith, S.L., 1989. Drift prospecting in the Appalachians of Estrie-Beauce, Québec. In: DiLabio, R.N.W., Coker, W.B. (Eds.), *Drift Prospecting*. Paper 89-20. Geol. Survey, Canada, pp. 41–59.
- Smedley, P.L., Kinniburgh, D.G., 2002. A review of the source, behavior and distribution of As in natural waters. *Appl. Geochem.* 17, 517–568.
- Smedley, P.L., Knudsen, J., Maiga, D., 2007. Arsenic in groundwater from mineralised Proterozoic basement rocks of Burkina Faso. *Appl. Geochem.* 22, 1074–1092.
- Środoń, J., Drits, V.A., McCarty, D.K., Hsieh, J.C.C., Eberl, D.D., 2001. Quantitative X-ray diffraction of clay-bearing rocks from random preparations. *Clays Clay Miner.* 49, 514–528.
- Stanley, R.S., Ratcliffe, N.M., 1985. Tectonic synthesis of the Taconian Orogeny in western New England. *Geol. Soc. Am. Bull.* 96, 1227–1250.
- Stewart, D.P., MacClintock, P., 1969. The Surficial Geology and Pleistocene History of Vermont. *Vermont Geol. Survey Bull.* #31.
- Sulkowski, M., Hirner, A.V., 2006. Element fractionation by sequential extraction in a soil with high carbonate content. *Appl. Geochem.* 21, 16–28.
- Sullivan, C.M., 2007. Evaluation of a Potential Ultramafic Source of Arsenic Contamination in Bedrock Water Wells in Central Vermont. Unpublished Bachelors Thesis, Middlebury College, Middlebury, Vermont.
- Taylor, St.R., McLennan, S.M., 1995. *The Continental Crust: Its Composition and Evolution*. Blackwell Scientific Publications, Oxford.
- Van Baalen, M., Francis, C., Mossman, B., 1999. Mineralogy, petrology and health issues at the ultramafic complex, Belvidere Mountain, Vermont, USA. In: *Guidebook to Field Trips in Vermont and Adjacent Regions of New Hampshire and New York: 91st Ann. New England Intercollegiate Geological Conf.*, Burlington, Vermont.
- Verplanck, P.L., Mueller, S.H., Goldfarb, R.J., Nordstrom, D.K., Youcha, E.K., 2008. Geochemical controls of elevated arsenic concentrations in groundwater, Ester Dome, Fairbanks district, Alaska. *Chem. Geol.* 255, 160–172.
- Wang, Y., Morin, G., Ona-Nguema, G., Menguy, N., Juillot, F., Aubry, E., Guyot, F., Calas, G., Brown Jr., G.E., 2008. Arsenite sorption at the magnetite-water interface during aqueous precipitation of magnetite: EXAFS evidence for a new arsenite surface complex. *Geochim. Cosmochim. Acta* 72, 2573–2586.
- Wedepohl, K.H., 1978. *Handbook of Geochemistry*. Springer-Verlag, Berlin–New York.